

Vacuum Decay Induced by Quantum Fluctuations

Haiyun Huang^{1,*} and L. H. Ford^{1,†}

¹*Institute of Cosmology, Department of Physics and Astronomy*

Tufts University, Medford, Massachusetts 02155, USA

Abstract

We treat the effects of quantum field fluctuations on the decay of a meta-stable state of a self-coupled scalar field. We consider two varieties of field fluctuations and their potential effects in a semiclassical description. The first are the fluctuations of the time derivative a free massive scalar field operator, which has been averaged over finite regions of space and time. These fluctuations obey a Gaussian probability distribution. A sufficiently large fluctuation is assumed to produce an effect analogous to a classical initial field velocity, which can cause a finite region to fly over the barrier separating the meta-stable state from the stable vacuum state. Here we find a contribution to the decay rate which is comparable to the decay rate by quantum tunneling, as computed in an instanton approximation. This result is consistent with those of other authors. We next consider the effects of the fluctuations of operators which are quadratic in the time derivative of the free scalar field. The quadratic operator is also averaged over finite regions of space and of time. Now the probability distribution for the averaged operator falls more slowly than an exponential function, allowing for the possibility of very large fluctuations. We find a contribution to the decay rate which is much larger than those coming from either quantum tunneling or linear field fluctuations, and hence appears to be the dominant decay mechanism.

*Electronic address: haiyun.huang@tufts.edu

†Electronic address: ford@cosmos.phy.tufts.edu

I. INTRODUCTION

Quantum tunneling is a well known effect in quantum mechanics. For example, a quantum particle in a local potential minimum has a nonzero probability to tunnel through a potential maximum to reach another potential minimum with lower energy. In many cases, the tunneling amplitude may be accurately calculated using the WKB approximation. However, there can be quantum field theoretic corrections to the tunneling rate calculated in single particle quantum mechanics. If the particle has an electric charge, it will respond to vacuum fluctuations of the electric field, which will result in a small increase in the tunneling rate [1, 2]. This increase arises from a one-loop correction to the tree level scattering amplitude, which here could be the WKB tunneling amplitude. If the particle is an electron, then this correction is described by the one-loop vertex diagram in quantum electrodynamics. However, as was discussed in Ref. [2], the increase in tunneling rate may be reasonably estimated from a simple semiclassical argument. The particle is subjected to vacuum electric field fluctuations even if no real photons are present. These fluctuations exert a force on the particle which can either push the particle toward the barrier, enhancing the tunneling probability, or away from the barrier, suppressing tunneling. However, the average effect is a small enhancement of the tunneling rate, in agreement with the one-loop perturbation theory calculation.

Vacuum radiation pressure fluctuations can also enhance the tunneling rate, and were studied in Ref. [3]. Here the enhancement is potentially much larger, and can possibly even dominate over the effect predicted by the WKB approximation. The type of large vacuum fluctuation will be discussed in more detail below in Sect. V.

The topic of the present paper will be role of quantum field fluctuations in the decay of a false vacuum state in field theory. Consider a real scalar field, $\phi(\mathbf{x}, t)$, with self-coupling described by a potential, $U(\phi)$, which has at least two local minima. If we quantize small perturbations around the global minimum, the ground state of the resulting field theory is called the true vacuum, whereas if we select a minimum with higher energy, the corresponding state is called a false vacuum, and is potentially unstable against decay into the true vacuum. A Euclidean space formalism which describes this decay by quantum tunneling was developed by Coleman [4], and will be reviewed in Sect. II. This formalism assumes an instanton approximation, in which the path integral for the tunneling amplitude is dominated by the single solution with smallest Euclidean action. It is very difficult to assess the accuracy of this approximation, which ignores the contributions of an infinite number of solutions, each of which individually may give a smaller contribution than that of the instanton, but collectively could give a larger effect. It was shown in Ref. [5] that the sum of all small perturbations around the instanton solution gives a subdominant effect, but this gives no information about the effects of very different decay mechanisms. Some examples of such mechanisms will be presented here.

The outline of this paper is as follows: Section II will review false vacuum decay by quantum tunneling, as described in the instanton approximation. Section III will discuss the classical dynamics of a self-coupled scalar field with two local potential minima, and illustrate how suitable initial conditions on the time derivative $\dot{\phi}$ of the classical field can cause a finite region to fly over the potential maximum separating these minima. In Sect. IV, we consider the effects of the vacuum fluctuations of the linear field operator, $\dot{\phi}(\mathbf{x}, t)$, averaged over a finite spacetime region, and argue that this effect can be of the same order as the instanton contribution to the decay rate. A similar conclusion was reached some time

ago by Linde [6], who studied the effects of ϕ fluctuations in de Sitter spacetime. After an early version of our results was first presented [7], we become aware of the work of several authors [8–11], who treat either ϕ or $\dot{\phi}$ fluctuations in either Minkowski or de Sitter spacetime, and also conclude that the contribution to the decay rate is of the same order as the instanton contribution. However, these authors disagree as to whether linear quantum field fluctuations and instanton methods are different formalisms for describing the same physical process, or whether they describe physically distinct processes. This is a question to which we will return later in this paper. Section V will discuss the fluctuations of a spacetime average of the quadratic operator $\dot{\phi}^2$. We argue that because the probability distribution for such an operator can fall more slowly than an exponential function [12–15], the effects of $\dot{\phi}^2$ fluctuations on the decay rate of the false vacuum can be much larger than either quantum tunneling, as described by an instanton, or the effects of linear field fluctuations. Our results are summarized and discussed in Sect. VI

Units in which $\hbar = c = 1$ will be used throughout this paper.

II. THE INSTANTON APPROACH TO FALSE VACUUM DECAY

In this section, we summarize the instanton method used by Coleman [4] to estimate the rate of false vacuum decay. Consider a real scalar field with the Lagrangian density

$$\mathcal{L} = \frac{1}{2}\partial_\mu\phi\partial^\mu\phi + U(\phi), \quad (1)$$

where $U(\phi)$ is a “double well” potential with two minima. The associated equation for $\phi(\mathbf{x}, t)$ is

$$\square\phi - U'(\phi) = 0, \quad (2)$$

where \square denotes the d’Alembertian operator in Lorentzian space [where we use metric signature $(-, +, +, +)$], and the four-dimensional Laplacian in Euclidean space. A specific choice for $U(\phi)$ is

$$U(\phi) = \frac{\lambda}{8}(\phi^2 - a^2)^2 + \frac{\epsilon\lambda a^3}{2}(\phi - a), \quad (3)$$

where λ , a , and ϵ are positive real constants. This form is illustrated in Fig. 1 for the case

$$\lambda = 0.01, \quad a = 1000, \quad \epsilon = 0.1. \quad (4)$$

The potential has a local minimum at $\phi = \phi_+$, the false vacuum, and a global minimum at $\phi = \phi_-$, the true vacuum. These minima are separated by a local maximum at $\phi = \phi_m$. For the choice of parameters given in Eq. (4) and illustrated in Fig. 1, $\phi_- \approx -1046.7$, $\phi_m \approx 101.0$, and $\phi_+ \approx 945.6$.

If the system is initially in the false vacuum state, we expect it to be unstable to decay to the true vacuum. In principle, the decay rate may be computed in the path integral formalism as

$$\Gamma \sim \sum_{\phi(x)} \exp(-S_E[\phi]), \quad (5)$$

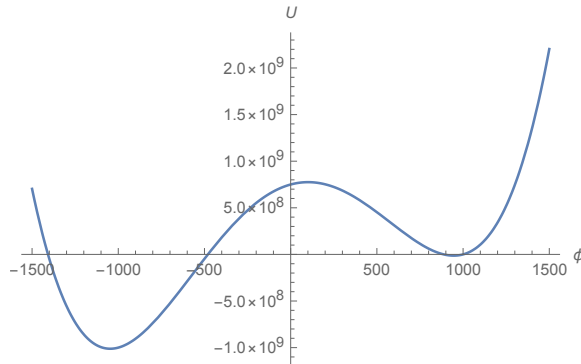


FIG. 1: The potential $U(\phi)$ given in Eq. (3) is plotted with the choice of parameters in Eq. (4).

where $\phi(x)$ is a field configuration in Euclidean space which approaches both ϕ_+ and ϕ_- in different limits. Here S_E is the Euclidean action, given by

$$S_E[\phi] = \int dt_E d\vec{x} \left[\frac{1}{2} \left(\frac{\partial \phi}{\partial t_E} \right)^2 + \frac{1}{2} (\vec{\nabla} \phi)^2 + U \right], \quad (6)$$

where the Wick rotation $t_E = it$ has been performed. The summation in Eq. (5) requires a sum over configurations $\phi(x)$, which cannot be computed exactly by any known methods. The instanton approximation assumes that this sum is dominated by the single solution of the Euclidean version of Eq. (2) with the lowest Euclidean action. Coleman calls this the “bounce” solution, for which $S_E = B$. In the instanton approximation, the decay rate becomes

$$\Gamma \approx e^{-B}. \quad (7)$$

Strictly, Γ is a probability rather than a decay rate. In order to infer a rate, we need to identify a characteristic time scale associated with the system. Then the decay rate is Γ divided by this time scale. This is analogous to the calculation of the decay rate of a radioactive nucleus by α -particle emission. One assume that the nucleus may be modeled as a metastable potential well, across which the α -particle moves on a time scale τ . Each time it reaches the boundary of the well, it has a probability Γ of tunneling through the barrier, leading to a decay rate of Γ/τ .

The bounce solution is assumed to be $O(4)$ symmetric, and hence Eq. (2) becomes an ordinary differential equation with independent variable $\rho = (t_E^2 + |\mathbf{x}|^2)^{1/2}$, the radius in four-dimensional Euclidean space. Here $t_E = it$ is the Euclidean time. This equation can be integrated numerically. We do this using the software package described in Ref. [16]. The result for the case of the parameters given in Eq. (4) is illustrated in Fig. 2. This solution describes the nucleation of a bubble filled with the true vacuum, which nucleates in the false vacuum with an initial radius of $\rho = \rho_0 \approx 0.275$. The bounce action in this case is

$$B \approx 2.47 \times 10^6. \quad (8)$$

The function $\phi(\rho)$ describes the spatial configuration of the bubble when it nucleates, with ϕ varying from the false vacuum value in the interior of the bubble to the true vacuum value on the exterior. The wall of the bubble is the region where ϕ varies most rapidly with increasing ρ . After nucleation, the bubble expands, with ρ taking the Lorentzian form, $\rho = (|\mathbf{x}|^2 - t^2)^{1/2}$.

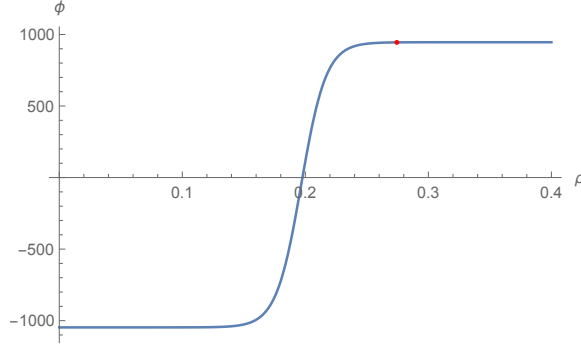


FIG. 2: The bounce solution $\phi(\rho)$ for the potential given in Eq. (3) with the choice of parameters in Eq. (4). Here $\phi(0) = \phi_-$ and $\phi(\rho) \rightarrow \phi_+$ as $\rho \rightarrow \infty$.

Thus the expansion of the wall of the bubble is described by a spacetime hyperbola, which is the world line of a uniformly accelerated particle. The expansion requires that the volume energy on the interior of the bubble at least balance the surface energy in the wall. As the bubble expands, the volume energy decreases due to the lower energy density of the true vacuum relative to the false vacuum, while the surface energy arising from spatial gradients in the wall increases. Bubbles with radii less than the minimum value, ρ_0 , will collapse rather than expand. This is similar to nucleation of bubbles of vapor in a boiling liquid.

There is one limit in which the bounce solution may be obtained analytically, when $\epsilon \ll 1$. In this case, called the thin-wall approximation, it is shown in Ref. [4] that the initial radius of the bubble is

$$\rho_{0tw} = \frac{2}{3\epsilon a \sqrt{\lambda}}, \quad (9)$$

and the bounce action is

$$B_{tw} = \frac{\pi^2}{6\epsilon^3 \lambda}. \quad (10)$$

Note that the parameter ϵ is defined differently in Ref. [4] from our definition. There the potential is written in the form

$$U(\phi) = \frac{\lambda}{8}(\phi^2 - a^2)^2 + \frac{\epsilon_1}{2a}(\phi - a), \quad (11)$$

where $\epsilon_1 = \epsilon \lambda a^4$, when ϵ is defined as in Eq. (3). For the choice of parameters in Eq. (4), one finds $\rho_{0tw} = 0.067$ and $B_{tw} = 1.63 \times 10^5$, which are not especially close to the numerical results quoted above. Apparently, $\epsilon = 0.1$ is not small enough for the thin wall approximation to be very accurate. As its name implies, the thin wall approximation requires that the wall thickness be small compared to the initial radius, which is not very accurately satisfied for the configuration illustrated in Fig. 2.

III. CLASSICAL FIELD DYNAMICS

A. Energy Conservation

Consider a real classical field ϕ which satisfies the equation of motion Eq. (2) in Minkowski spacetime, so

$$\square\phi = -\partial_t^2\phi + \nabla^2\phi = U'(\phi). \quad (12)$$

The associated energy density of this field is

$$T_{tt} = \frac{1}{2}[(\partial_t\phi)^2 + |\nabla\phi|^2] + U(\phi). \quad (13)$$

Consider a finite spatial region R , and define the field energy in this region at time t by

$$E_R(t) = \int_R d^3x T_{tt}(\mathbf{x}, t). \quad (14)$$

Then

$$\frac{dE_R}{dt} = \int_R d^3x \{ \partial_t\phi [\partial_t^2\phi + U'(\phi)] + \nabla\phi \cdot \nabla\partial_t\phi \} = \int_R d^3x \{ \partial_t\phi [\partial_t^2\phi - \nabla^2\phi + U'(\phi)] + \nabla \cdot (\partial_t\phi \nabla\phi) \}. \quad (15)$$

The last term in the above expression is a total divergence, which may be written as a surface integral over the boundary S of region R :

$$\int_R d^3x \nabla \cdot (\partial_t\phi \nabla\phi) = \oint_S d\mathbf{S} \cdot (\partial_t\phi \nabla\phi), \quad (16)$$

which will vanish if either $\partial_t\phi$ or the normal component of $\nabla\phi$ vanish on each point of S . In this case, Eqs. (12) and (15) imply that E_R is a constant.

In the case of a spatially homogeneous field, $\phi = \phi(t)$, the spatial integration simply produces a constant factor of the volume of R , and $E_R \propto (\dot{\phi})^2/2 + U(\phi(t))$. This is of the same form as the energy of a point particle in a potential. The turning points of the motion occur when $U(\phi)$ reaches its maximum value, and $\dot{\phi} = 0$. The case of an inhomogeneous field is somewhat more complicated, but one can still approximately identify turning points as occurring when $\int_R d^3x U(\phi(t)) \approx E_R$, when the contributions of both $(\dot{\phi})^2$ and $|\nabla\phi|^2$ to E_R are small. Thus if the variation of ϕ within R is small compared to the variation between a pair of turning points of $U(\phi)$, we can view R as a localized region which moves between these turning points much as does a point particle.

B. Motion over a Barrier

Consider the dynamics of a finite region in a potential with local minima, such as illustrated in Fig. 1. If the energy E_R of the region is small, then the motion is expected to be confined to be near one minimum, analogous to that of a classical particle oscillating about a minimum. However, larger values of E_R might allow the region to pass over the local maximum. One way to achieve this would be to impose initial conditions that $\phi = \phi_+$ and $\dot{\phi} = \dot{\phi}_0 \neq 0$ in a finite spatial region R . If $|\dot{\phi}_0|$ and the size of R are sufficiently large, then

this region can move over the local maximum at ϕ_m to the global minimum at $\phi = \phi_-$. In the potential illustrated in Fig. 1, this can happen more easily if $\dot{\phi}_0 < 0$. This would be a classical version of quantum false vacuum decay. The region R becomes a bubble similar to those discussed in Sect. II. Again, there is a competition between the volume energy inside the bubble and surface energy in the wall, which requires that the bubble have a minimum size before it can expand rather than collapse. If the bubble does expand, it eventually fills all of space with a region where $\phi \approx \phi_-$, the global minimum. This will be illustrated in some numerical simulations in Sect. IV C 2. In the next section, we discuss a model where the classical initial condition on $\dot{\phi}_0$ is replaced by the effect of a quantum field fluctuation.

IV. VACUUM DECAY INDUCED BY $\dot{\phi}$ FLUCTUATIONS

In this section, we will be concerned with possible effects of the quantum fluctuations of the scalar field, ϕ , and its space and time derivatives, such as $\dot{\phi}$. We assume that $\phi \approx \phi_+$, the false vacuum value, and that to leading order, ϕ is a linear quantum field with mass m .

A. The Probability Distribution for Spacetime Averaged $\dot{\phi}$ Fluctuations

The fluctuations of a field operator at a single spacetime point are not meaningful, but averages over space and/or time are well defined. We can view these averages as the result of a measurement of the field in a finite region. Here we consider averaging over both space and time regions and write the average of $\dot{\phi}$ as

$$\bar{\dot{\phi}} = \int dt f(t) \int d^3x g(\mathbf{x}) \dot{\phi}(\mathbf{x}, t), \quad (17)$$

where the averaging functions are normalized by

$$\int dt f(t) = \int d^3x g(\mathbf{x}) = 1. \quad (18)$$

The probability distribution for $\bar{\dot{\phi}}$ fluctuations in the vacuum state is a Gaussian function,

$$P(\bar{\dot{\phi}}) = \frac{1}{\sqrt{2\pi\sigma^2}} \exp\left(-\frac{\bar{\dot{\phi}}^2}{2\sigma^2}\right), \quad (19)$$

where the variance σ^2 is

$$\sigma^2 = \langle \bar{\dot{\phi}}^2 \rangle = \langle 0 | \int dt_1 d^3x_1 f(t_1) g(\mathbf{x}_1) \dot{\phi}(t_1, \mathbf{x}_1) \int dt_2 d^3x_2 f(t_2) g(\mathbf{x}_2) \dot{\phi}(t_2, \mathbf{x}_2) | 0 \rangle. \quad (20)$$

We may write the linear operator $\dot{\phi}$ as

$$\dot{\phi}(x) = \sum_{\mathbf{k}} \sqrt{\frac{\omega}{2V}} [e^{i(\mathbf{k}\cdot\mathbf{x}-\omega t)} a_{\mathbf{k}} + e^{-i(\mathbf{k}\cdot\mathbf{x}-\omega t)} a_{\mathbf{k}}^\dagger], \quad (21)$$

where V is a quantization volume, and $\omega^2 = k^2 + m^2$. This leads to an expression for the variance:

$$\sigma^2 = \frac{1}{2(2\pi)^3} \int d^3k \, \omega \, |\hat{g}(\mathbf{k})|^2 |\hat{f}(\omega)|^2, \quad (22)$$

where $\hat{f}(\omega)$ and $\hat{g}(\mathbf{k})$ are the Fourier transforms of the time and space sampling functions, respectively. We assume that $\tau \neq 0$ is the characteristic width of $f(t)$, and hence is the time sampling interval. Similarly, let $\ell \neq 0$ be the characteristic spatial sampling interval. It is convenient to define dimensionless functions with unit sampling intervals by

$$f_1(t) = \frac{1}{\tau} f\left(\frac{t}{\tau}\right), \quad g_1(\mathbf{x}) = \frac{1}{\ell^3} g\left(\frac{\mathbf{x}}{\ell}\right). \quad (23)$$

Let \hat{f}_1 and \hat{g}_1 be their corresponding Fourier transforms. We can now express the variance as

$$\sigma^2 = \frac{\eta}{2\ell^3\tau}, \quad (24)$$

where

$$\eta := \frac{1}{(2\pi)^3} \int d^3\kappa \, \Omega \, |\hat{g}_1(\boldsymbol{\kappa})|^2 |\hat{f}_1(\Omega)|^2, \quad (25)$$

with $\Omega^2 = \kappa^2 \frac{\tau^2}{\ell^2} + m^2 \tau^2$. Note that η is a dimensionless constant which depends upon the functional forms of the sampling functions, as well as the dimensionless constants ℓ/τ and $m\tau$.

B. Compactly supported functions

We adopt the view that the sampling functions $f(t)$ and $g(\mathbf{x})$ should have compact support, meaning that they are strictly equal to zero outside of finite intervals. The physical motivation for this is that these functions should describe measurements made within finite time intervals and spatial regions. A temporal sampling function such as a Gaussian or Lorentzian has tails which extend into the past and the future, and strictly describes a measurement which began in the infinite past and continues into the infinite future. A better choice is an infinitely differentiable function with compact support. Such functions have Fourier transforms which fall faster than any power, but more slowly than an exponential function. A class of these functions was discussed in Refs [13] and [15], and have Fourier transforms with the asymptotic forms

$$\hat{f}(\omega) \sim \exp[-(\omega\tau)^\alpha], \quad \hat{g}(k) \sim \exp[-(k\ell)^\lambda], \quad (26)$$

where α and λ are real constants which satisfy $0 < \lambda \leq \alpha < 1$. Here the spatial sampling function is assumed to be spherically symmetric, so $g = g(r)$ and $\hat{g} = \hat{g}(k)$. The coordinate space switch-on or switch-off behavior is linked to the values of α and λ . For example, if $f(t)$ switches on at $t = 0$, then it might have the form

$$f(t) \sim D t^{-\mu} \exp(-w t^{-\nu}) \quad (27)$$

as $t \rightarrow 0^+$ for some constants D , μ , w , and ν . The most important of these is ν , which is related to the parameter α in f by $\nu = \alpha/(1 - \alpha)$. The choice $\alpha = 1/2$, where $\nu = 1$, has special physical interest, as there is an electrical circuit which switches on with this behavior [13]. Some explicit examples of compactly supported functions were given in Sect. IIB of Ref. [13] and in Appendix A of Ref. [15].

Another choice can be given in coordinate space by

$$f_1(t) = C_f \begin{cases} \exp\left(-\frac{1}{1-t^2}\right), & t \in [-1, 1] \\ 0, & t < -1 \text{ or } t > 1 \end{cases} \quad (28)$$

and

$$g_1(\vec{x}) = C_g \begin{cases} \exp\left(-\frac{1}{1-|\vec{x}|^2}\right), & |\vec{x}| \in [-1, 1] \\ 0, & |\vec{x}| < -1 \text{ or } |\vec{x}| > 1, \end{cases} \quad (29)$$

where C_f and C_g are normalization factors chosen so that Eq. (18) holds. The functions above correspond to $\alpha = \lambda = 1/2$, and $\tau = \ell = 1$.

C. Effects of Large $\bar{\phi}$ Fluctuations

Let us return to the process described in Sect. IIIB, where a classical initial condition on $\dot{\phi}$ could cause a finite spatial region to move from the false vacuum, over the barrier to the true vacuum. However, we now consider quantum vacuum fluctuation of a space and time average, $\bar{\phi}$, and ask under what conditions it might produce the same effect. The probability of a sufficiently large fluctuation may be estimated from Eqs. (19) and (24) once we have estimates for $\bar{\phi}$, τ , ℓ and η . We expect that we need $\frac{1}{2}\bar{\phi}^2 \gtrsim \Delta U$, where

$$\Delta U = U(\phi_0) - U(\phi_F) \quad (30)$$

is the height of the potential barrier above the false vacuum level. Take the minimum value of the magnitude of $\dot{\phi}$ to be

$$|\dot{\phi}_0| = (2\Delta U)^{\frac{1}{2}}. \quad (31)$$

Let the minimum value of τ be

$$\tau_0 = \frac{\Delta\phi}{|\dot{\phi}_0|}, \quad (32)$$

where $\Delta\phi = |\phi_0 - \phi_F|$. That is, τ_0 is the time that would be required for the field to change by $\Delta\phi$ if it maintained an average speed of $\dot{\phi}_0$. Finally, we estimate that the minimum size of the spatial averaging region should be of the order of the radius at which a bubble could nucleate in the given potential,

$$\ell_0 \approx \rho_0. \quad (33)$$

Recall that this is the minimum radius at which the internal pressure can balance the tension in the bubble wall. More generally, we expect the values of $\dot{\phi}$, τ , and ℓ to be of the order of the minimum values estimated above. Set

$$\dot{\phi} = V \dot{\phi}_0, \quad \tau = T \tau_0, \quad \ell = L \ell_0, \quad (34)$$

where V , T , and L are constants of order unity.

Let

$$A = \frac{\bar{\phi}^2 \ell^3 \tau}{\eta} = V^2 L^3 T \frac{\bar{\phi}_0^2 \ell_0^3 \tau_0}{\eta}. \quad (35)$$

If $A < B$, then

$$P(\bar{\phi}) > \Gamma \approx e^{-B}, \quad (36)$$

and the effect of $\bar{\phi}$ fluctuations on false vacuum decay will dominate over quantum tunneling in the instanton approximation.

1. Thin Wall Case

Here we wish to compare estimates of A with B in the thin wall approximation. Take the example of the potential given in Eq. (3) for the case $\epsilon \ll 1$. To lowest order in ϵ , we have $\phi_F \approx a$, $\phi_0 \approx 0$, and $\Delta U \approx \frac{1}{8} \lambda a^4$, leading to

$$\dot{\phi}_0 \approx \frac{1}{2} \sqrt{\lambda} a^2, \quad \tau_0 \approx \frac{2}{\sqrt{\lambda} a}. \quad (37)$$

If we combine these estimates with $\ell_0 \approx \rho_{0tw}$ and Eq. (9), we find

$$A \approx \frac{4 V^2 L^3 T}{27 \eta \epsilon^3 \lambda}. \quad (38)$$

Comparison with Eq. (10) shows that $A < B$ and hence quantum $\bar{\phi}$ fluctuations dominate over quantum tunneling in the thin wall limit if

$$\frac{\eta}{V^2 L^3 T} > \frac{8}{9 \pi^2} \approx 0.090. \quad (39)$$

The value of η depends upon the choices of the sampling functions $f(t)$ and $g(\mathbf{x})$, but can be expected to be of order one, in which case Eq. (39) will be satisfied if $V^2 L^3 T$ is not too large.

2. Numerical Simulations

Here we describe some numerical integrations of Eq. (12) with $U(\phi)$ as given in Eqs. (3) and (4). The initial condition is that $\phi(0) = \phi_+$ everywhere and that $\dot{\phi}(0)$ is a negative constant within a sphere of initial radius ℓ . The numerical solution, $\phi(t, r)$ is inspected to check that at least the region near $r = 0$ has passed through $\phi = \phi_m$ and reached $\phi \approx \phi_-$. If so, this describes a bubble of true vacuum surrounded by false vacuum formed by a $\bar{\phi}$. However, a quantum fluctuation is transient and its energy must be given up on some timescale $\tau = T\tau_0$. We model this effect by stopping the numerical integration at $t = \tau$, and then restarting it with a new initial condition that $\phi(t = \tau, r)$ has the value found in the previous part of the integration, but $\dot{\phi}(t = \tau, r) = 0$. That is, the value of $\dot{\phi}$ is set to

zero for the beginning of the second part of the simulation. Equation (12) is now further integrated with these initial conditions at $t = \tau$ to see if the bubble continues to expand.

The first part of the simulation for the case $L = 1$, $V = 1.15$, and $T = 3$ is illustrated in Fig. 3, and the second part in Fig. 4. The vertical plane in Fig. 3 corresponds to $t = \tau = 3\tau_0$, when the first part ends. By this time, the center of the bubble is in the true vacuum phase. Figure 4 illustrates the bubble expanding at close to the speed of light, with true vacuum in the interior, and false vacuum on the exterior.

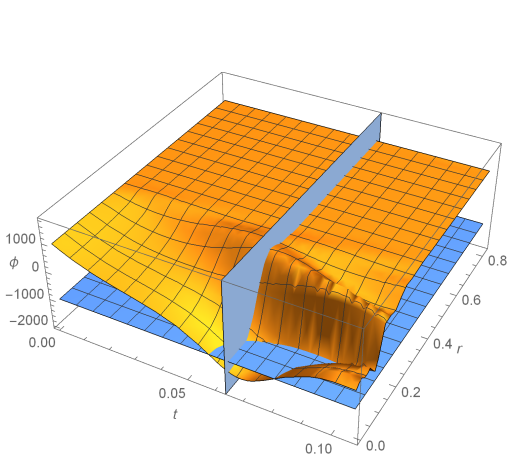


FIG. 3: The first part of the simulation, for the fluctuation in the case $L = 1$, $V = 1.15$, $T = 3$.

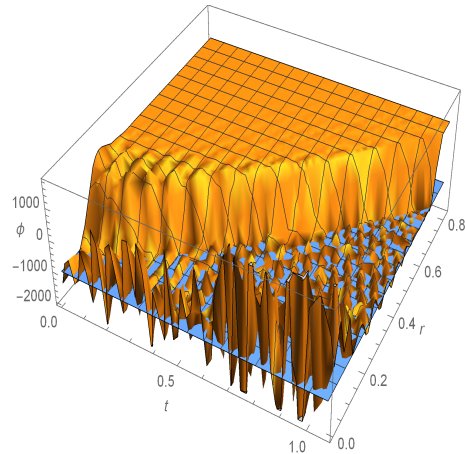


FIG. 4: The succeeding second part of the simulation, following Fig. 3.

For some choices of the parameters, the bubble fails to expand in the second part of the simulation, but rather collapses. Here the internal pressure due to the true vacuum energy is unable to overcome the wall tension. One such case is illustrated in Fig. 5.

Table I lists the results found with several choices of the parameters L , T , and V , along with the values of A and A/B . In general, A/B is roughly of order unity, indicating roughly comparable contributions from $\bar{\phi}$ fluctuations and from quantum tunneling in the instanton approximation. However, in several cases we find $A/B < 1$, suggesting that $\bar{\phi}$ fluctuations can give a larger contribution to the decay rate.

Note that the typical values of τ are a few times $1/m$, which is also of the order of the oscillation period in the quadratic potential $m^2 \phi^2/2$, which approximates $U(\phi)$ near the false vacuum. We can take τ as defining the characteristic time scale which convert a probability into a decay rate, so this rate becomes approximately $P(\bar{\phi})/\tau$.

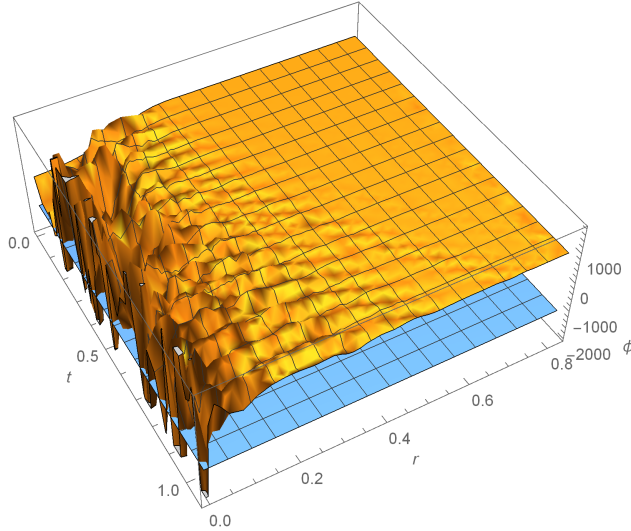


FIG. 5: The second step of the simulation for the case $L = 1; T = 1.5; V = 1.15$. The region of true vacuum fails to expand out.

V. VACUUM DECAY INDUCED BY QUADRATIC OPERATOR FLUCTUATIONS

A. Probability Distributions

In the previous section, we discussed the possibility that vacuum fluctuations of a linear operator, such as the spacetime average of ϕ , could induce decay of the false vacuum. Now we turn to the effects of the fluctuations of a quadratic operator, such as $\dot{\phi}^2$. The probability distributions for such operators have been treated in Refs. [12–15]. Just as is the case for $\dot{\phi}$, a quadratic operator must also be averaged in spacetime before a meaningful probability distribution can be defined. Recall that for a linear operator, the averaging could be over only time or only space, although we selected averaging in both as being more physically realistic. The averaging of a quadratic operator must be in time, as spatial averaging alone does not suffice. As before, we consider a spacetime average. A key result is that the probability distribution for an averaged quadratic operator, such as $\overline{\dot{\phi}^2}$, falls more slowly than exponentially for large fluctuations. This means that large fluctuations of $\dot{\phi}^2$ and similar operators are more likely than one might expect, and hence may have larger physical effects than linear operator fluctuations.

Consider the case of a space and time average of normal ordered $:\dot{\phi}^2:$,

$$\overline{\dot{\phi}^2} = \int dt f(t) \int d^3x g(\mathbf{x}) : \dot{\phi}^2(\mathbf{x}, t) :, \quad (40)$$

where we again take $f(t)$ and $g(\mathbf{x})$ to be functions with compact support whose Fourier transforms have the asymptotic forms given in Eq. (26). It is shown in Ref. [15] that when

TABLE I: The comparison between the two mechanisms of vacuum decay, for the potential barrier of $\lambda = 0.01, a = 1000, \epsilon = 0.1$, under different fluctuations.

| Trial | L | T | V | Expands out? | ℓ/τ | $m\tau$ | η | A | A/B |
|-------|-----|-----|------|--------------|-------------|---------|-----------|-----------------------|-----------|
| 1 | 1 | 3 | 1.15 | ✓ | 4.30309 | 5.85342 | 0.132452 | 2.08004×10^7 | 8.41474 |
| 2 | 1 | 2.5 | 1.15 | ✓ | 5.16371 | 4.87785 | 0.0328028 | 6.99902×10^7 | 28.3143 |
| 3 | 1 | 2 | 1.15 | ✓ | 6.45464 | 3.90228 | 0.392158 | 4.68357×10^6 | 1.89472 |
| 4 | 1 | 1.6 | 1.15 | ✓ | 8.0683 | 3.12182 | 2.00058 | 734468. | 0.297127 |
| 5 | 1 | 1.5 | 1.15 | × | 8.60619 | 2.92671 | 2.81314 | 512466. | 0.207316 |
| 6 | 1.1 | 1.5 | 1.15 | ✓ | 9.46681 | 2.92671 | 2.81314 | 651759. | 0.263667 |
| 7 | 1.1 | 1.2 | 1.15 | ✓ | 11.8335 | 2.34137 | 5.66249 | 259036. | 0.104792 |
| 8 | 1.1 | 1.1 | 1.15 | ✓ | 12.9093 | 2.14625 | 6.824 | 197033. | 0.0797092 |
| 9 | 1 | 1 | 1.15 | × | 14.2002 | 1.95114 | 7.88181 | 116515. | 0.0471358 |
| 10 | 1 | 1.5 | 1.1 | ✓ | 9.46681 | 2.92671 | 2.68803 | 468872. | 0.189681 |

$\lambda \leq \alpha < 1$, the probability distribution for $\overline{\dot{\phi}^2}$ has the asymptotic forms,

$$P(\overline{\dot{\phi}^2}) \sim \exp[-a_1(\tau^2 \ell^2 \overline{\dot{\phi}^2})^\alpha], \quad (41)$$

when $\ell \lesssim \tau$, and

$$P(\overline{\dot{\phi}^2}) \sim \exp[-a_2(\ell^4 \overline{\dot{\phi}^2})^\alpha], \quad (42)$$

when $\ell \gtrsim \tau$. Here a_1 and a_2 are constants of order unity. Note that both $\tau^2 \ell^2 \overline{\dot{\phi}^2}$ and $\ell^4 \overline{\dot{\phi}^2}$ are dimensionless measures of the magnitude of $\overline{\dot{\phi}^2}$. The above asymptotic forms hold when the arguments of the exponentials are large compared to one.

Note that it is the parameter α associated with $f(t)$ which governs the probability of large fluctuations. Because $\alpha < 1$, comparison of Eq. (19) with either of Eq. (41) or Eq. (42) shows that the probability of a large $\overline{\dot{\phi}^2}$ fluctuation can be much greater than that of the corresponding $\overline{\dot{\phi}}$ fluctuation for which $\overline{\dot{\phi}^2} = \overline{\dot{\phi}}^2$.

B. Effects of Large $\overline{\dot{\phi}^2}$ Fluctuations

We saw in Sect. IV C that the vacuum fluctuations of $\overline{\dot{\phi}}$ can produce a contribution to false vacuum decay which is comparable to the instanton contribution. Further, we have just seen that the probability of a $\overline{\dot{\phi}^2}$ fluctuation can be much larger than that of a comparable $\overline{\dot{\phi}}$ fluctuation. This implies that the effects of the fluctuations of quadratic operators, such $\overline{\dot{\phi}^2}$

can dominate both instanton and $\overline{\dot{\phi}^2}$ fluctuation effects. They can potentially also dominate over finite temperature effects, which satisfy a Boltzmann probability distribution and can be described by a sphaleron [17, 18]. Here a thermal fluctuation causes a finite region to go over the potential barrier.

Let $D = \ell^4 \dot{\phi}^2$. If $\ell \gtrsim \tau$ and $D \gg 1$, then Eq. (42) becomes approximately

$$P(\overline{\dot{\phi}^2}) \sim e^{-D^\alpha} \quad (43)$$

if we set $a_2 \approx 1$. Comparison with Eq. (7) shows that $\overline{\dot{\phi}^2}$ fluctuations dominate if $D^\alpha < B$. We can illustrate this dominance with an explicit example. Consider Trials 1-4 listed in Table I. In all of these cases, one finds $D \approx 1.18 \times 10^7$ if $\overline{\dot{\phi}^2} = \overline{\dot{\phi}^2}$. Note that A , which depends upon τ in addition to $\overline{\dot{\phi}^2}$, varies among these trials. Recall that here $B \approx 2.47 \times 10^6$, so we will have $D^\alpha < B$ if $\alpha \lesssim 0.904$, which includes the greater part of the allowed range $0 < \alpha < 1$. In particular, if $\alpha = 1/2$, we have $D^\alpha/B \approx 0.0014$, so $\overline{\dot{\phi}^2}$ fluctuations will greatly dominate the instanton contribution to the decay rate.

C. Measurement of $\overline{\dot{\phi}^2}$

In this subsection, we will describe a thought experiment by which an averaged quadratic operator such as $\overline{\dot{\phi}^2}$ could be measured in a compact region of spacetime. Consider the Raychaudhuri equation for the expansion θ of a bundle of timelike geodesics:

$$\frac{d\theta}{d\tau} = -R_{\mu\nu} u^\mu u^\nu, \quad (44)$$

where $R_{\mu\nu}$ is the Ricci tensor, u^μ is the four-velocity of a particle on a geodesic, and τ is its proper time. Here we have assumed that terms involving θ^2 or the squares of the shear or vorticity may be neglected. If we measure the change in the expansion of the bundle, $\Delta\theta$, averaged over finite intervals of time and space, then we have measured certain components an averaged Ricci tensor, $\overline{R_{\mu\nu}}$, averaged with compactly supported sampling functions $f(t)$ and $g(\mathbf{x})$ defined by the details of the geodesic bundles. By varying the the four-velocity, u^μ , we can potentially obtain all of the diagonal components of $\overline{R_{\mu\nu}}$. Next we may infer the averaged components of the stress tensor from the Einstein equation in the form

$$\overline{T_{\mu\nu}} = \frac{1}{8\pi G} (\overline{R_{\mu\nu}} - \frac{1}{2} \overline{R}), \quad (45)$$

where G is Newton's constant and $R = R^\mu{}_\mu$.

Now we assume that the source of the gravitational field is the self-coupled scalar field with Lagrangian density given in Eq. (1), for which the stress tensor is

$$T_{\mu\nu} = \partial_\mu \phi \partial_\nu \phi - \frac{1}{2} g_{\mu\nu} \partial^\rho \phi \partial_\rho \phi - g_{\mu\nu} U(\phi). \quad (46)$$

Further assume that the gravitational field is weak, and that in the above expression we may take the metric to have the Minkowski form $g_{\mu\nu} \approx \eta_{\mu\nu} = \text{diag}(-1, 1, 1, 1)$. If we form a particular combination of the components of $T_{\mu\nu}$, the potential $U(\phi)$ cancels, and we have

$$3T_{tt} + T_{xx} + T_{yy} + T_{zz} = 3\dot{\phi}^2 + |\nabla\phi|^2. \quad (47)$$

We expect $\dot{\phi}^2$ and $|\nabla\phi|^2$ to be of the same order of magnitude, so measurements of $\overline{R_{\mu\nu}}$, and hence of $\overline{T_{\mu\nu}}$, allow us to obtain an estimate of $\overline{\dot{\phi}^2}$.

D. What determines α ?

We have seen that the probability distributions for the fluctuations of quadratic operators, such as $\overline{\dot{\phi}^2}$, are very sensitive to the parameter α defined in Eq. (26). This parameter determines the rate of decrease of $\hat{f}(\omega)$, the Fourier transform of the temporal sampling function $f(t)$, and is also linked to the switch-on and switch-off behavior of $f(t)$. In the measurement of $\overline{\dot{\phi}^2}$ described in the previous subsection, α will be determined by the details of the bundles of test particles used. The more rapidly these bundles begin and end, the smaller will be α , and hence the larger the likely value of $\overline{\dot{\phi}^2}$ obtained in the measurement. This seems to imply that if we measure $\overline{\dot{\phi}^2}$ in the false vacuum state with bundles with small α , the probability of immediate decay is much greater than if we had use a larger value of α . This issue needs further study, as it is not immediately clear why a purely gravitational measurement should perturb the scalar field theory so much.

Another open question is what effect will fluctuations have upon the false vacuum in the apparent absence of a measurement of the form described above. It is possible that the dynamics of coupling of the quantum field fluctuations with the classical background scalar field can determine a specific value of α , but how this might happen is unclear.

VI. SUMMARY AND CONCLUSIONS

In this paper, we have discussed the effects of linear and quadratic quantum field fluctuations on the decay rate of a false vacuum of a self-coupled scalar field. This rate is usually computed in an instanton approximation, where the solution of lowest Euclidean action is assumed to dominate a path integral. We first consider the effects of the vacuum fluctuations of a linear field, ϕ , averaged over finite intervals of both space and time. We have argued that this averaging describes a physical process or measurement which necessarily begins and ends at finite times, and occurs in compact regions of space and time. Hence the averaging should be described by infinitely differentiable, but compactly supported and hence non-analytic functions of space and time. A quantum $\dot{\phi}$ fluctuation in a finite region has an effect similar to a classical initial field velocity, and if its magnitude is large enough, can cause a finite region to fly over a potential barrier, in a manner similar to the motion of a classical particle.

We find that quantum $\dot{\phi}$ fluctuations can cause false vacuum decay at a rate which is comparable to the rate of quantum tunneling, as described in the instanton approximation. This is consistent with the conclusions in Refs [6, 8–11], although these authors offer differing conclusions as to whether linear quantum field fluctuations are an alternative formalism for describing quantum tunneling, or represents a distinct physical process. We adopt the latter viewpoint. Evidence that $\dot{\phi}$ fluctuations are a separate decay channel from tunneling arises in the dependence of the variance in Eqs. (24) and (25) upon the sampling functions. Our view is that these functions should be determined by the physical details of the system, here perhaps the dynamics of the formation of the bubble of true vacuum.

This dependence is even more pronounced in the case of the effects of quadratic quantum field fluctuations, such as $\overline{\dot{\phi}^2}$, upon the decay rate. Here we found an effect which can significantly dominate over quantum tunneling. This arises because the probability distribution, $P(\overline{\dot{\phi}^2})$, falls more slowly than an exponential function when compactly supported averaging functions are used, and provides strong evidence that $\overline{\dot{\phi}^2}$ fluctuations provide a different decay process than quantum tunneling.

Acknowledgments

We would like to thank Mark Hertzberg, Ken Olum, Alex Vilenkin, Shao-Jiang Wang, and Masaki Yamada for helpful discussions. We also thank Ali Masoumi for providing the software package described in Ref. [16], and assistance in its use. This work was supported in part by the National Science Foundation under Grant PHY-1912545.

-
- [1] V.V Flambaum and V.G. Zelevinsky, Radiation corrections increase tunneling probability, *Phys. Rev. Lett.* **83**, 3108 (1999), arXiv:nucl-th/9812076.
 - [2] H. Huang and L. H. Ford, Quantum electric field fluctuations and potential scattering, *Phys. Rev. D* **91**, 125005 (2015), arXiv:1503.02962.
 - [3] H. Huang and L. H. Ford, Vacuum radiation pressure fluctuations and barrier penetration, *Phys. Rev. D* **96**, 016003 (2017), arXiv:1610.01252.
 - [4] S. Coleman, Fate of the false vacuum: Semiclassical theory, *Phys. Rev. D* **15**, 2929 (1977).
 - [5] C. G. Callan and S. Coleman, Fate of the false vacuum II: First quantum corrections, *Phys. Rev. D* **16**, 1762 (1977).
 - [6] A. Linde, Hard art of universe creation, *Nucl. Phys.* **B372**, 421 (1992), hep-th/910037.
 - [7] H. Huang, False vacuum decay and quantum fluctuations, seminar at Tufts University, April 19, 2018.
 - [8] J. Braden, M. C. Johnson, H. V. Peiris, A. Pontzen, and S. Weinfurtner, A new semiclassical picture of vacuum decay, *Phys. Rev. Lett.* **123**, 031601 (2019), arXiv:1806.06069.
 - [9] M. P. Hertzberg and M. Yamada, Vacuum decay in real time and imaginary time formalisms, *Phys. Rev. D* **100**, 016011 (2019), arXiv:1904.08565.
 - [10] J. J. Blanco-Pillado, H. Deng, and A. Vilenkin, Flyover vacuum decay, arXiv:19006.09657.
 - [11] S.-J. Wang, Occurrence of semiclassical vacuum decay, *Phys. Rev. D* **100**, 096019 (2019), arXiv:1909.11196.

- [12] C. J. Fewster, L. H. Ford, and T. A. Roman, Probability distributions for quantum stress tensors in four dimensions, *Phys. Rev. D* **85**, 125038 (2012), arXiv:1204.3570.
- [13] C. J. Fewster and L. H. Ford, Probability distributions for quantum stress tensors measured in a finite time interval, *Phys. Rev. D* **92**, 105008 (2015), arXiv:1508.02359.
- [14] E. D. Schiappacse, C. J. Fewster and L. H. Ford, Vacuum quantum stress tensor fluctuations: A diagonalization approach, *Phys. Rev. D* **97**, 025013 (2018);, arXiv:1711.09477.
- [15] C. J. Fewster and L. H. Ford, Probability distributions for space and time averaged quantum stress tensors, *Phys. Rev. D* **101**, 025006 (2020), arXiv:1909.07285.
- [16] A. Masoumi, K. Olum, and B. Shlaer, Efficient numerical solution to vacuum decay with many fields, *JCAP* **01** 051 (2017), arXiv:1610.06594.
- [17] F. R. Klinkhamer and N.S. Manton, A saddle-point solution in the Weinberg-Salam theory, *Phys. Rev. D* **30**, 2212 (1984).
- [18] P. Arnold and L. McLerran, Sphalerons, small fluctuations, and baryon-number violation in electroweak theory, *Phys. Rev. D* **36**, 581 (1987); The sphaleron strikes back: A response to objections to the sphaleron approximation, *Phys. Rev. D* **37**, 1020 (1988).